ISSN: 2277-9655
Impact Factor: 3.785

IJESRT

INTERNATIONAL JOURNAL OF ENGINEERING SCIENCES & RESEARCH TECHNOLOGY

MICROSTRUCTURE, PHASE TRANSFORMATIONS AND MECHANICAL PROPERTIES OF SOLUTION TREATED BI-MODAL β TITANIUM ALLOY

Nader El-Bagoury*, Khaled M. Ibrahim

* Chemistry Department, Faculty of Science, TAIF University, PO Box 888, El-Haweyah, El-Taif, Saudi Arabia.

Casting Technology Lab, Manufacturing Technology Department, CMRDI, PO Box 87, Helwan, Cairo, Egypt.

Taibah University, College of Engineering, P.O. Box. 344 Al-Madinah Al-Mounwara, Saudi Arabia.

DOI: 10.5281/zenodo.51527

ABSTRACT

The effect of heat treatment conditions on the microstructure, phase transformation and mechanical properties of Bi-modal β titanium alloy was investigated. The heat treatment process comprises of solution treated at various temperatures of 640, 680, 720 and 760 °C for 30 min followed by water quenching and aged at 500 °C for 30 min then air cooling. This study was carried out using X-ray diffraction analysis (XRD), scanning electron microscope (SEM), energy dispersive spectrometer (EDS), differential thermal analysis (DTA), compression universal testing machine and Vickers hardness tester. The results show that the microstructure of investigated alloys consists of β phase, as a matrix, primary α phase, small precipitates of secondary α phase in addition to orthorhombic martensite (α") phase found only in the solutionized samples at 720 and 760 °C. Transus temperature for the β phase found to be around 865 °C at heating rate of 10 °C/min. The α/β phase zone is ranging from 650 to 865 °C at the same heating rate for all samples. The formation temperature of nanometer α phase and/or disappearing of ω_{iso} phase are almost constant at 385 °C. The formation of primary α phase was detected at a temperature more than 400 °C. Hardness measurements increased as the solution temperature increase. The highest ultimate compression strength, 2680 MPa, achieved with solution temperature of 680 °C. However the maximum yield stress, 1725 MPa, obtained with 760 °C solution temperature. The highest contraction was attained with the solutionized sample at 640 °C for 30 min.

KEYWORDS: Bi-modal titanium alloy, solution treatment, α-β structure, compression strength, hardness.

INTRODUCTION

Titanium alloys exhibit mechanical and physical properties which fit aerospace applications in which light weight, good wear and corrosion resistance are required. This category of alloys provides significant economic benefit in these applications. However, these unique properties are strongly affected by the chemical composition, microstructure, deformation and heat treatment conditions [1, 2].

Despite these advantages, the use of titanium alloys was often slowed down owing to their cost with respect to other materials. To overcome this difficulty, new processing routes are developed. This is the case for the new TIMETAL Ti LCB (for low cost beta) that presents a lower cost compared to other Ti alloys by using an inexpensive Fe-Mo master alloy widely used in the steel industry. New applications then emerged, particularly in the automotive industry (suspension springs) [3].

Depending on their chemical composition, titanium alloys have α, α + β or β microstructure. Predominately, parts are manufactured from two-phase alloys α + β [4, 5]. According to the literature, it shows the complexity of issues concerning the microstructure- mechanical properties relationships in titanium alloys [6–10]. The fine and coarse grained structures of α + β titanium alloys are controlled by the chemical composition, melting and casting methods, plastic deformation, and heat treatment processes.

ISSN: 2277-9655
Impact Factor: 3.785

In this work the influence of heat treatment conditions on the microstructure, phase transformations and mechanical properties of Bi-Modal β Titanium alloy will be studied.

EXPERIMENTAL WORK

A vacuum induction furnace was used to melt and cast bi-modal β titanium alloy as rods of 30 mm in diameter and 300 mm length. Hot swaging was applied to these rods at 760 °C, in the range of α+β zone, to reduce the cross-section diameter from 25 mm to 10 mm in 11 steps. The chemical composition of the studied bi-modal β titanium alloy and molybdenum and aluminum equivalents, $[Mo]_{eq}$ and $[Al]_{eq}$ are listed in Table 1. Small-sized parts were taken from the swaged alloy to be used as samples in the heat treatment processes. These samples were solution treated at 640, 680, 720 and 760 °C for 30 min followed by water quenching (WQ). Ageing processes were applied at 500 °C for 30 min before air cooling (AC), as shown in Table 2. The metallographic specimens for the microstructure examination were prepared according to ASTM E3 [11] then etched in a solution of 10 ml HF and 5 ml HNO_3 and 85 ml H_2O (Kroll's reagent). Microstructural studies using scanning electron microscopy (SEM - JEOL JSM5410) were conducted. The equilibrium phase composition was detected by an energy X-ray dispersive spectroscopy (EDS) attached to SEM. The XRD analyses for the crystalline phases in the investigated samples were carried out on the Brucker axis D8 diffractometer. The samples were measured in step scan mode with steps of 0.02° 2θ of range 30–45° using Cu Ka (λ= 1.5406) as applied radiation. The phase transformations of the studied samples were measured by Netzsch CC 200 F1 differential thermal analysis (DTA) with a cooling/heating rate of 10 °C/min in the temperature range from 25 to 1000 °C. Hardness values were determined using Leco Vickers Hardness Tester LV800AT with 10 Kg_f. The compression tests with samples ϕ 10 mm × 15mm were performed using computer controlled electro-hydraulic servo universal testing machine WAW-300 (SN. 010816), which manufactured by Jinan testing equipment IE Corporation, at a cross-head displacement speed of 0.01 mm/min.

Table 1. Chemical composition of bi-modal β titanium alloy.

Chemical composition (wt%)						
Al	**Mo**	**Fe**	**O**	**Ti**	**$[Mo]_{eq}$**	**$[Al]_{eq}$**
2.49	3.74	4.63	0.142	Bal.	14.677	3.91

Table 2. Symbol and heat treatment conditions for investigated samples.

Symbol	**Heat treatment conditions**	
	Solution treatment	**Aging treatment**
Sample A	640 °C/ 30 min	500 °C/30 min
Sample B	680 °C/ 30 min	
Sample C	720 °C/ 30 min	
Sample D	780 °C/ 30 min	

RESULTS AND DISCUSSION

X- Ray Diffraction

In order to characterize the phase transformation during the heat treatment processes for bi-modal Ti alloys, X-ray diffraction (XRD) technique was used. XRD was carried out for four samples solutionized at 640, 680, 720 and 760 °C for 30 min at room temperatures. XRD patterns for different phases; such as β, α and α'' can be seen in Fig. 1. This figure presents the position and intensity of various phases that can be found in the microstructures of the investigated samples. The volume fractions of the phases are directly proportional to the integrated intensity of their specific diffraction peaks. The main peak of 100 β phase is visible at 2θ equal to 39.75° in both A and B solutionized samples at 640 and 680 °C. However, there is a shift of this peak to lower values of 2θ. For example for C sample there was a slight decrease in 2θ to 39.72°, while a remarkable shift in 2θ was accompanied to D sample found at 39.42° [12]. Reflections 100, 020, 002 and 101 related to α phase were found in all four studied samples. Moreover, 100, 110, 020, 002 and 111 peaks of orthorhombic α" martensite appeared only with higher solution temperature samples; (C and D) and not in lower solution temperature samples; (A and B), as shown in Fig. 1.

ISSN: 2277-9655
Impact Factor: 3.785

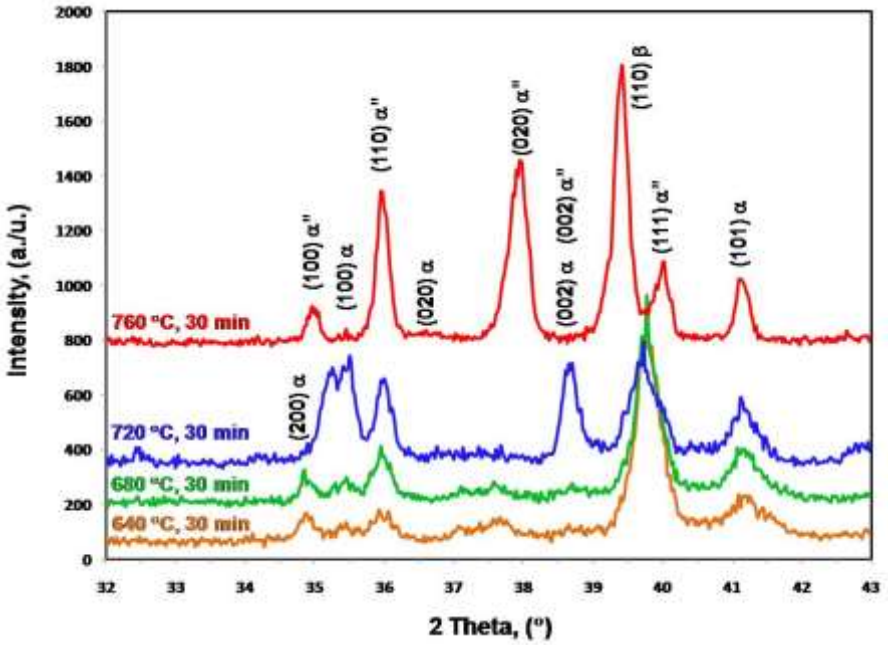

Fig. 1 X-ray diffraction pattern of investigated bi-modal titanium samples.

Microstructure Evolution

The microstructure evolution during heat treatment processes is influenced by the previous applied conditions such as plastic deformation, history of the materials (initial microstructure and chemistry). Alloy under investigation was swaged at first at 760 °C below the β-transus temperature, T_β, (α+β zone) producing a bi-modal microstructure of primary α phase and β matrix [13].

Figure 2 shows the microstructure of the investigated samples heat treated with various conditions. The microstructure of the A sample, solutionized at 640 °C, consists of the hexagonal close packed (hcp) primary α phase (black), and secondary small α precipitates imbedded in β (bcc) matrix, as illustrated in Fig. 2 (a) [14, 15]. The volume fraction (V_f) of the globular α phase is about 32%, in sample A. Some of the primary α phase found in the microstructure in lamellar shape. Increasing the solution temperature to 680 °C, the microstructure of sample B contains the same constitutes as in the sample A, but in different percentages [16]. Where the V_f of primary α phase decreased to approximately 25% and the V_f of secondary α precipitates lowered as well, Fig. 2 (b). The microstructure of sample C has coarser primary α phase in comparison with the previous alloys in about 18% V_f and smaller percentage of secondary α precipitates, illustrated in Fig. 2 (c). Some colonies of orthorhombic martensite (α") phase, in small percentages, could exist in the microstructure of this alloy, as confirmed by the XRD measurements, as shown in Fig. 1. At highest solution temperature of 760 °C, the microstructure of sample D forms of a remarkable blocky primary α phase with the lowest V_f of about 14%. Moreover, the secondary α phase that dispersed in matrix is almost disappeared from this microstructure, depicted in Fig. 2 (d).

In the microstructure of sample D, where solution temperature is 760 °C, orthorhombic martensite phase (α") is found in this microstructure, in higher percentage than in sample C, as shown in Fig. 3 (a), which is confirmed by XRD, see Fig. 1. Moreover, at highest solution temperature, platelet α phase as well as grain boundary α (GB α) are formed in the microstructure of Alloy D as depicted in Fig. 3 (b).

Table 3 shows the chemical composition of primary α (α_p) and β phases. It is clear that α_p phase has higher Al content than β phase where Al is α stabilizer. However, β phase has higher contents of Mo and Fe than in α phase as both of these elements considered β phase stabilizer [16]. Additionally, the distribution of these alloying elements, Al, Mo

and Fe, among different phases is shown in Fig. 4 using line analysis technique by EDS unit attached in SEM. Both of Ti and Al elements preferably segregate to α phase while Mo and Fe selectively distributed to β phase as illustrated in Fig. 4.

Table 3. Chemical composition of α_p and β phases in sample C.

Phase	Chemical composition, at%			
	Al	Mo	Fe	Ti
α_p	3.57	0.90	1.60	Bal.
β	2.70	4.93	3.52	Bal.

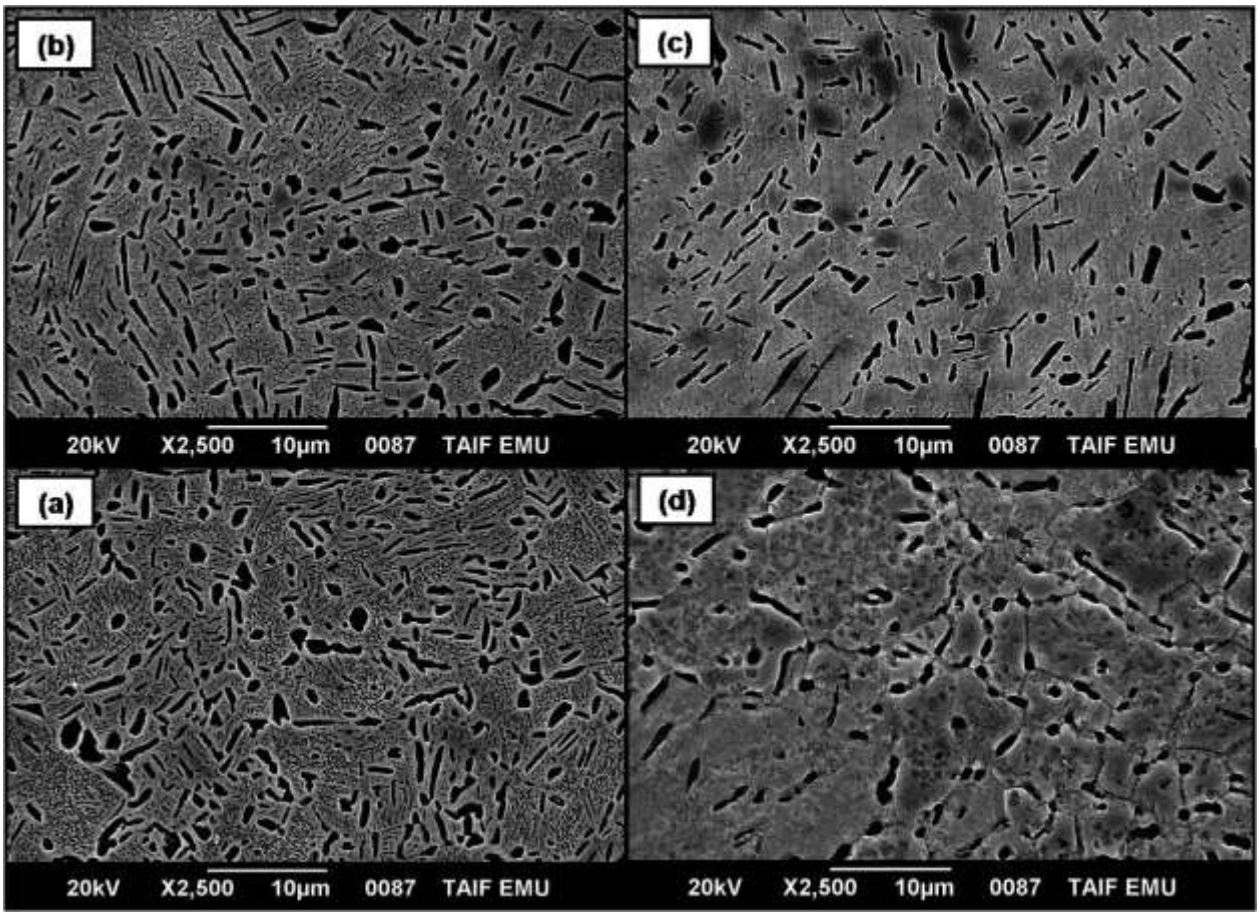

Fig. 2 Microstructure of heat treated samples (a) 640 ℃, (b) 680 ℃, (c) 720 ℃ and (d) 760 ℃.

ISSN: 2277-9655
Impact Factor: 3.785

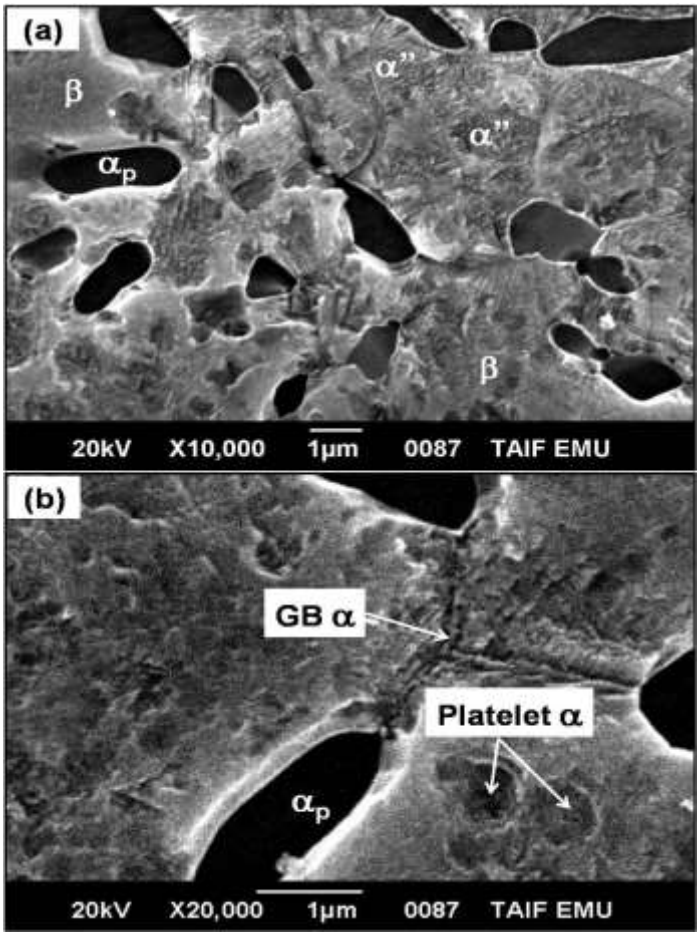

Fig. 3 Microstructure of 760 ℃ for 30 min Ti alloy (a) α, β and α" phases (b) grain boundary and platelet α phases.

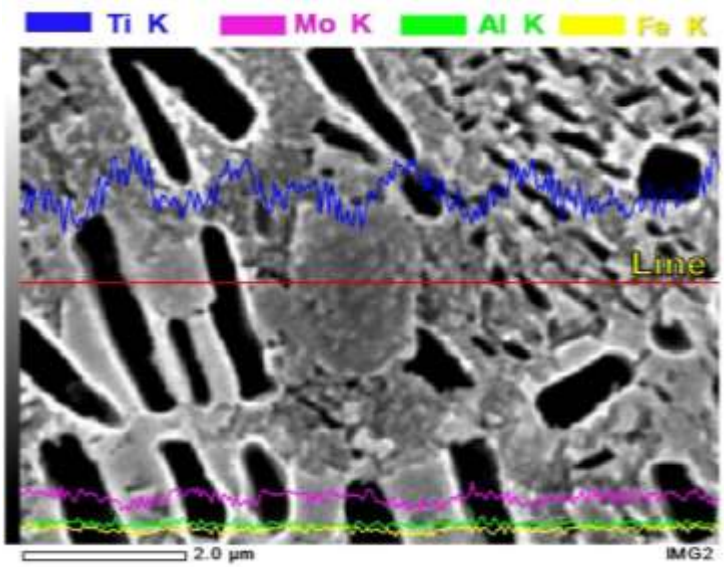

Fig. 4 Line analysis of different phases in 680 ℃ for 30 min Ti alloy.

Differential Thermal Analysis

Table 4 lists the results of differential thermal analysis (DTA) for all investigated samples including various phase transformation temperatures. The DTA curves obtained for sample B during heating at rate of 10 °C/min are shown in Figure 5.

There are various important peaks obtained by the DTA experiments such as ω_{iso}^{*}, $\omega_{iso}/\alpha_{nano}$, α, α", α/β and T_{β}, as shown in Table 4.

Table 4. The DTA experimental results for the investigated samples at 10 ℃/min.

Sample	Peak 1	Peak 2	Peak 3	Peak 4	Peak 5	Peak 6
	ω_{iso}	$\omega_{iso}/\alpha_{nano}$	α	α"	α/β	T_{β}
A	300.1	384.9	411.1	--	642.3	816.5
B	283.8	385.8	411.7	--	650.9	865.4
C	275.2	386.9	410.5	439.7	646.9	872.0
D	305.3	377.6	404.8	443.5	656.7	856.3

ω_{iso}: Precipitation of omega phase.
$\omega_{iso}/\alpha_{nano}$: Disappearance of omega phase or precipitation of alpha phase.
α: Formation of alpha phase
α": Formation of orthorhombic martensite phase.
α/β: Alpha plates formation in beta phase.
T_{β}: Transus of beta phase.

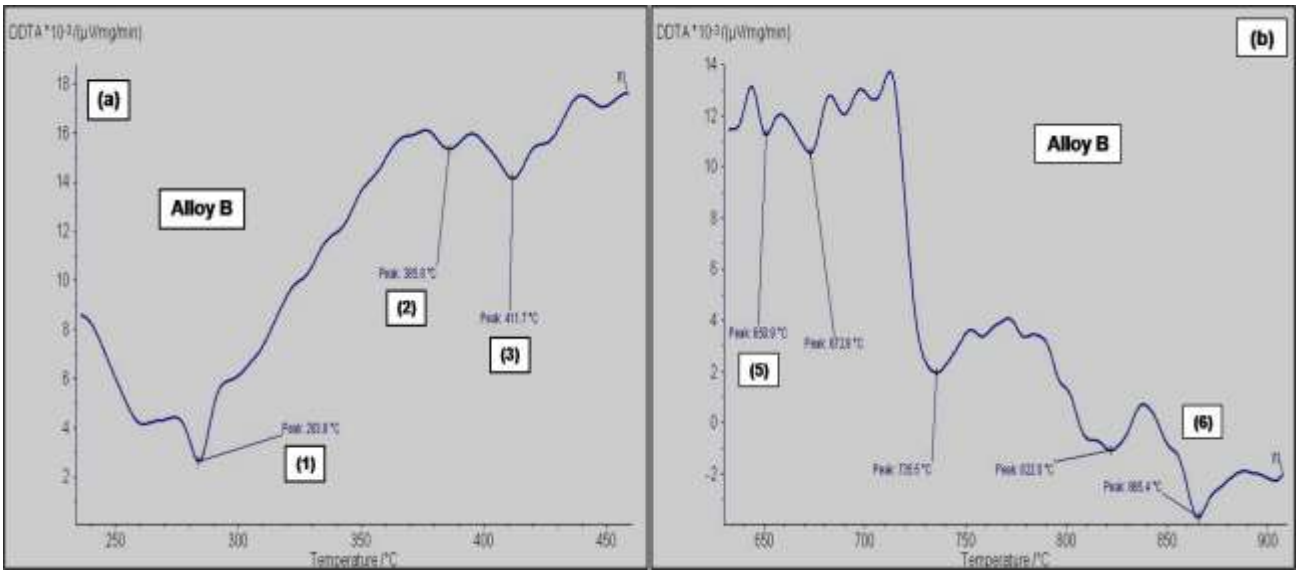

Fig. 5 DTA curves for sample B at heating rate of 10 ℃/min.

According to Prima [17] who reported on the phase transformation in LCB Ti alloy with 2 °C/min heating rate, there are four domains related to the experimental observations. The first domain; is correlated to the dissolution of ω_{ath} (athermal omega phase in the range of room temperature to 200 °C). Domain two; is related to the precipitation of ω_{iso} (isothermal omega phase in the range of 200 to 350 °C; peak 1). The third domain belongs to the disappearance or coalescence of ω_{iso} and /or the precipitation of nano-particles of alpha phase (from 350 to 400 °C; peak 2). The last domain represents the formation of globular alpha phase (at 480 °C). Orthorhombic martensite phase (α") was confirmed by Bruneseaux et al. [18]. The precipitation of the α" phase was evidence between 350 and 450 °C at

heating rate of 6°C/min [17]. As the T_β transus is known to be near 865°C, the α/β phase field is ranging from about 650°C to 860°C (α/β transformation) [12, 19].

According to the result of this study, the α" phase found only in the DTA curves of sample C and D (solutionized at 720 and 760 °C) at 439.7 and 443.5 °C, respectively at heating rate of 10 °C/min, as shown in Table 4. Moreover, it is worth noting that the precipitation of ω_{iso} phase is inversely related to the solution treatment temperature. Whereas the solution treatment temperature increases from 640 to 680, 720 and 760 °C, the transformation temperature of ω_{iso} phase decreases from 300.1 to 283.8, 275.2 and 245.0 °C, respectively, as shown in Table 4. The former results could originate from the redistribution and more homogeneous chemical composition for higher solution temperatures.

The formation temperature of nanometer α phase and/or disappearance of ω_{iso} phase are almost constant at 385 °C in all solution treatment conditions except in case of sample D, which is 305.3 °C. Additionally, the formation temperature of α phase is a little bit more than 400 °C except in sample C, which has the highest temperature of 439.7 °C. Typically as obtained by Quentin et. al., [12] the transus temperature recorded in this study is around 865 °C in all studied samples but sample A has the lowest temperature of 816.5 °C.

Mechanical Properties

Table 5 summarizes the mechanical properties of the four A, B, C and D samples. This table contains the ultimate compressive strength (UCS), yield stress, modules of elasticity (E), contraction (C) and hardness (Hv_{10}) of the studied samples. The shape of investigated alloys after carrying out the compression test is shown in Fig. 6. The microstructure affects the mechanical properties especially strengthening of β phase, primary α phase and fine secondary precipitates of α particles and transformed martensite phase (α").

Table 5. Mechanical properties of investigated samples at room temperature.

Sample	E (GPa)	$\sigma_{0.2}$ (MPa)	UCS (MPa)	C (%)	Hv_{10}
A	51.39	640	1275	11.8	352
B	83.39	1380	2680	11.6	368
C	109.44	1485	2355	9.2	399
D	101.63	1725	2100	6.5	431

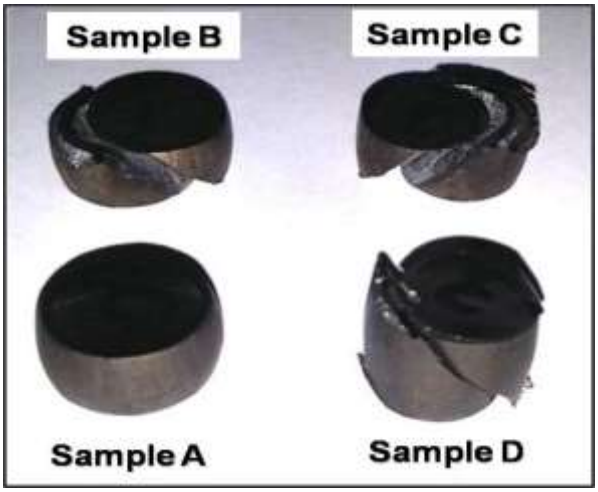

Fig. 6 Photographs of investigated samples after compression test.

Sample A has the highest percentage of contraction, 11.8 %, among other alloys as shown in Table 5. Additionally, according to that higher ductility, sample A had not fractured entirely like the others. However, instead it swelled containing internal cracks only. Helm [20] observed that the ductility of IMI 834 alloys was improved with higher

volume fraction of primary α phase. The highest V_f of primary α phase was obtained in the microstructure of sample A leading to highest ductility. The fracture modes of samples B, C and D are identified to be a typical shear fracture with a crack along the 45° angle of the specimens.

For the UCS, sample B has the highest value of 2680 MPa, while sample A got the lowest one. It seems that the microstructure of sample B has the best combination of volume fraction and size of primary and secondary α phases that strengthen the matrix of β phase, in the absence of orthorhombic martensite α" phase. However, the presence of α" in the microstructures of both C sample, lower percentage, and D sample with higher percentage, decreasing the UCT to 2355 and 2100 MPa, and lowering C% to 9.2 and 6.5, respectively [21]. Moreover, grain size has an influencing role on UCS where sample B has smaller α and β grain size in comparison with samples C and D [22].
Hardness measurements have a direct relationship with the elevation in solution temperature. Sample D has the highest value of hardness while sample A has the lowest one. The prevailing cause of these results could be due to the increase in the V_f of the orthorhombic martensite phase α" with the increase in temperature of solution treatment process. Yield stress, just like hardness, increases as the solution temperature increases. This is attributed to the secondary α precipitation strengthening effect, which is much stronger in comparison with the grain size strengthening effect [23]. The maximum modules of elasticity, 109.44 GPa, was obtained with solution treatment temperatures of 720 °C then slightly decreased to 101.63 GPa with 760 °C.

CONCLUSION

[1] The microstructure of the studied samples is consists of β matrix, primary α phase and fine particles of secondary α phase precipitated in the matrix of β.
[2] Orthorhombic martensite α" phase was found only in the microstructures of sample C and sample D solutionized at 720 and 760 °C, respectively, for 30 min.
[3] The temperature of nano α phase formation is around 385 °C; however, the transformation temperature of primary α phase is taken place at 411 °C.
[4] The transformation temperature range of α/β region is located between 650 and 865 °C. The β phase transus is represented by the latter temperature.
[5] The highest ultimate compression strength was achieved by solution treatment at 680 °C (sample B). Moreover, sample D has the maximum values for hardness and yield stress. However, maximum contraction was obtained by solution treatment at 640 °C for 30 min.

REFERENCES

[1] Titanium and Titanium Alloys. Fundamentals and applications, edited by C. Leyens, M. Peters (WILEY-VCH Verlag GmbH&Co.KGaA, Weinheim, 2003).
[2] V.N. Moiseyev, Titanium alloys: Russian aircraft and aerospace application, edited by J.N. Fridlyander (Taylor&Francis, USA, 2006).
[3] Schauerte O., Titanium in automotive production, Advanced Engineering Materials, vol. 5, No. 6, 411-418, 2003.
[4] Bylica A, Sieniawski J. Titanium and its alloys. Warszawa: PWN, 1985 (in Polish).
[5] SzkliniarzW. Possibilities of heat treatment application for grains refinement of titanium and titanium alloys. Hutnictwo, Wydawnictwo Politechniki S ´ la˛skiej, Gliwice (in Polish).
[6] Z.B. Zhou, Y. Fei, M.J. Lai, H.C. Kou, H. Chang, G.Q. Shang, Z.S. Zhu, J.S. Li, L. Zhou, Microstructure and mechanical properties of new metastable β type titanium alloy, Trans. Nonferrous Met. Soc. China Vol. 20, p.p. 2253-2258, 2010.
[7] Grewal G, Ankem S. Particle coarsening behavior of alpha–beta titanium alloys. Metall Trans A, Vol. 21, No. 6, p.p. 1645– 1654, 1990.
[8] Breslauer E, Rosen A. Relationship between microstructure and mechanical properties in metastable beta titanium 15– 3 alloy. Mater Sci Technol, Vol. 7, No. 5, p.p. 441– 446, 1991.
[9] Andres C, Gysler A, Luetjering G. Correlation between microstructure and creep behavior of the high temperature Ti alloy IMI 834. Z Metallkd, Vol. 88, No. 3, p.p. 197– 203, 1997.

[10] Ponsonnet L, Quesne C, Penelle R. Microstructure and creep deformation of a near beta titanium alloy beta-CEZ. Mater Sci Eng; Vol. A262, No. 1– 2 p.p. 50– 63, 1999.
[11] ASTM Standard E3. Standard Practice for Preparation of Metallographic Specimens, 1995.
[12] Quentin Contrepois, Marc Carton, Jacqueline Lecomte-Beckers, Characterization of the β Phase Decomposition in Ti-5Al-5Mo-5V-3Cr at Slow Heating Rates, *Open Journal of Metal*, Vol. 1: p.p. 1-11, 2011.
[13] MA F, LU W, QIN J, ZHANG D. Microstructure evolution of near-α titanium alloys during thermomechanical processing [J]. Materials Science and Engineering A, Vol. 416, p.p. 59−65, 2006.
[14] J. Sieniawski, Phase transformations and microstructure development in multicomponent titanium alloys containing Al, Mo, V and Cr, Oficyna Wydawnicza Politechniki Rzeszowskiej, Rzeszów, (1985). (in Polish).
[15] Lütjering G. Influence of processing on microstructure and mechanical properties of (+) titanium alloys. Materials Science and Engineering. Vol. A243, No. (1-2), p.p.32-45, 1998.
[16] Khaled M. Ibrahim, M. Mahmoud Moustafa, Mubarak W. Al-Grafi, Nader El-Bagoury, Mohammed A. Amin, Effect of Solution Heat Treatment on Microstructure and Wear and Corrosion Behavior of a Two Phase β-Metastable Titanium Alloy, 2016. Accepted in International Journal of Electrochemical Science.
[17] F. Prima, P. Vernaut, G. Texier, D. Ansel and T. Gloriant, "Evidence of A-nanophase Heterogeneous from Ω Particles in a β-metastable High-Resolution Electron Microscopy," Scripta Materi alia, Vol. 54, 2006, pp. 645-648.
[18] F. Bruneseaux, G. Geandier, E. Gauthier, B. Appolaire, M. Dehmas and P. Boulet, "In Situ Characterization of the Transformation Sequen Energy X-ray Diffraction: Infkuence of the Thermal Path," In: M. Nimoni, S. Akiyama, M. Ikeda, M. Hagi-wara, K. Maruyama, Eds., Ti-2007 Science and Technology, The Japan Institute, Vol. 1, 2007, pp. 563-566.
[19] Thierry Gloriant, G. Texier, F. Sun, I. Thibon, F. Prima, Jean-Louis Soubeyroux, Characterization of the nanophase precipitation in a metastable beta titanium-based alloy by electrical resistivity, dilatometry and neutron diffraction, Scripta Materialia, 2008, 58, pp.271-274.
[20] D. Helm. Application of Ti-alloys as compressor discs and blades. In *TMS*, pages 291-298, Warrendale, PA, USA, 1999. TMS - Miner. Metals & Mater. Soc.
[21] P.N. Zhang and J. Liu, Microstructure and mechanical properties in Co–Ni–Ga–Al shape memory alloys with two-phase structure, Journal of Alloys and Compounds 2008, 462, p.p. 225 -228.
[22] E. Lee, Microstructure Evolution and Microstructure/Mechanical Properties Relationship in α+β Titanium Alloys, Degree Doctor of Philosophy, The Ohio State University, 2004.
[23] A. Bhattacharjee, Vydehi A. Joshi, and A.K. Gogia. Effect of heat treatment on tensile behavior of a Ti-10V-2Fe-3Al alloy. In Titanium '99: Science and Technology, pages 529-535, 1999.